Journal of Civil Engineering and Management
ISSN 1392-3730 / eISSN 1822-3605
2021 Volume 27 Issue 8: 637–650
https://doi.org/10.3846/jcem.2021.14905

COMBINING EBR CFRP SHEET WITH PRESTRESSED NSM STEEL STRANDS TO ENHANCE THE STRUCTURAL BEHAVIOR OF PRESTRESSED CONCRETE BEAMS

M. OBAYDULLAH[1], Mohd Zamin JUMAAT[1], U. Johnson ALENGARAM[1*], Md. Humayun KABIR[2], Muhammad Harunur RASHID[2]

[1]*Centre for Innovative Construction Technology (CICT), Department of Civil Engineering, Faculty of Engineering, University of Malaya, 50603 Kuala Lumpur, Malaysia*
[2]*Department of Civil Engineering, Khulna University of Engineering and Technology, Khulna, Bangladesh*

Received 3 March 2021; accepted 25 March 2021

Abstract. In this study, a combined strengthening technique is used to improve the flexural performance of prestressed concrete beams using CFRP sheets as EBR and prestressed steel strands as NSM. Seven prestressed beams were tested under four-point loading with one control specimen, one EBR CFRP sheet strengthened specimen, one NSM steel strand without prestress strengthened specimen and four specimens strengthened with a combination of EBR CFRP sheet and NSM steel strands prestressed from 0% to 70% of their tensile strength. The flexural responses and failure modes of the specimens were investigated and the variations due to the level of prestressing force in the PNSM steel strands were also assessed. A finite element model (FEM) was developed using ABAQUS to verify the flexural responses of the strengthened specimens. The test results revealed that the combined strengthening technique remarkably enhanced the flexural performance of the specimens. The serviceability, first crack, yield, and ultimate load capacities improved up to 44%, 49%, 55% and 70%, respectively when compared with the control specimen. The combined technique also ensured the flexural failure of the specimens with significant enhancement in stiffness and energy absorption. The results of the FEM model exhibited excellent agreement with the experimental results.

Keywords: prestressed beams, flexural behavior, EBR, NSM, PNSM, Combined technique, CEBNSM, CEBPNSM, prestressed strengthening, FEM.

Introduction

Prestressed concrete (PC) has been used extensively in construction worldwide and faces challenges similar to reinforced concrete (RC) during construction and service, such as design errors, increasing traffic loads, environmental exposure, physical damage from vehicle accidents, etc., which may require structural strengthening (Lee et al., 2017). The most commonly used strengthening materials are CFRP and steel, and the most popular strengthening techniques are externally bonded reinforcement (EBR) (Attari et al., 2012) and near surface mounted (NSM) reinforcement (De Lorenzis & Nanni, 2001; El-Hacha & Rizkalla, 2004; Hosen et al., 2016; Darain et al., 2015). The key problems with EBR are environmental damage and premature failure (Brena et al., 2003). NSM was developed to overcome these drawbacks. However, NSM also has certain limitations (De Lorenzis & Teng, 2007) and does not completely eliminate the possibility of premature debonding failure (Al-Mahmoud et al., 2009; Sharaky et al., 2015).

Combining EBR and NSM (CEBNSM) is a recent advancement in structural strengthening which can enhance the effectiveness of strengthening and overcome some of the limitations of both techniques. Lim (2009) used a combination of EBR CFRP strips and NSM CFRP strips on nine RC T-beams. Flexural strength and stiffness significantly increased; however, failure occurred due to debonding of the EBR strips. Rahman et al. (2015) tested seven RC beams using a combination of EBR steel plates and NSM steel bars. The flexural capacity of the strengthened beams was enhanced, although failure still occurred by debonding. However, failure was significantly delayed due to improved bond performance. Darain (2016) investigated the structural behavior of six RC beams strengthened with a combination of EBR CFRP fabric and NSM

*Corresponding author. E-mail: *johnson@um.edu.my*

Copyright © 2021 The Author(s). Published by Vilnius Gediminas Technical University

This is an Open Access article distributed under the terms of the Creative Commons Attribution License (http://creativecommons.org/licenses/by/4.0/), which permits unrestricted use, distribution, and reproduction in any medium, provided the original author and source are credited.

CFRP bars. The flexural strength and stiffness were significantly enhanced and most of the beams failed flexurally.

Another strengthening technique is prestressing of EBR or NSM material to improve strengthening effectiveness and enhance overall flexural response. Prestressing provides various advantages, such as improved serviceability, delayed cracking and better utilization of strengthening materials, due to effects of cambering. A limited number of studies have been conducted on prestressed strengthening of PC beams. Casadei et al. (2006) strengthened two damaged PC beams, one with prestressed NSM (PNSM) CFRP bars and the other with EBR CFRP laminate, and found that both techniques restored the ultimate capacity. However, the PNSM CFRP beam displayed better structural behavior in terms of ductility and flexural failure, while the EBR beam failed by debonding. The researchers concluded that PNSM CFRP strengthening restored the full functionality of the prestressed beam. Reza Aram et al. (2008) tested four short PC beams to investigate the use of prestressed EBR CFRP strips for strengthening. However, no significant improvement in flexural behavior or strength was found, and the beams failed by premature debonding. The researchers concluded that prestressed strengthening may be more effective in long span beams than short beams. Obaydullah et al. (2016) investigated the use of PNSM steel strands on seven PC beams, with varying levels of prestress force in the strengthening reinforcement. The strengthened beams showed significant improvement in flexural strength and structural behavior at both service and ultimate stages, and the strengthened beams failed flexurally. Higher levels of prestress force resulted in better performance of the strengthened beams. The researchers further concluded that the use of steel strands for strengthening resulted in the ductile performance of the strengthened specimens comparable to the unstrengthened beam.

This present study proposes an innovative new strengthening technique which combines EBR with PNSM, namely the CEBPNSM technique. In this study, the strengthening of PC beams with the CEBPNSM technique is investigated using CFRP sheets as EBR reinforcement, due to certain superior properties such as resistance to corrosion and high strength to weight ratio, and prestressed steel strands as PNSM reinforcement due to their superior ductility, bond performance and high strength. The steel strands were protected from corrosion as they were embedded with epoxy in the NSM groove. The NSM steel strands were prestressed to various levels of prestress force to study the effect of higher levels of prestress on the structural performance of the strengthened beams. To the best of the researchers' knowledge, no such previous study has been conducted. The aim of this study is to develop the CEBPNSM technique as an efficient new strengthening solution to overcome the limitations of NSM and EBR, and provide a possible solution for structures that require higher levels of strengthening. A FEM model was also developed using ABAQUS to verify the flexural responses of the strengthened specimens.

1. Experimental program

1.1. Test matrix

The experimental investigation was conducted on seven PC beams. A reference specimen was kept unstrengthened, while one specimen was strengthened with an EBR CFRP sheet and another specimen with a NSM steel strand, for comparison purposes. The remaining four specimens were strengthened using the CEBNSM technique with EBR CFRP sheets and NSM steel strands. The steel strands were prestressed to 0%, 50%, 60% and 70% of the tensile strength of the strands. The experimental test matrix is shown in Table 1.

1.2. Prestressed beam specifications

The prestressed beams were 3300 mm long, 150 mm wide and 300 mm high, with an effective span of 3000 mm. The internal steel reinforcements were deformed 10 mm steel bars. Three 12.9 mm diameter prestressing strands were prestressed to 75% of their tensile capacity and placed in the compression and tension zone. The nominal concrete cover was 35 mm. The reinforcement details and beam dimensions are shown in Figure 1.

Table 1. Test matrix

Specimen ID	NSM strengthening materials			Prestressing level in NSM steel strands (% of tensile capacity)	EBR strengthening materials	
	Type	Diameter (mm)	Bond length (mm)		Type	Dimension (mm)
UB	Unstrengthened beam			–	–	–
EBR-Sh	–	–	–	–	CFRP Sheet	2900×100×0.17
NSM-S-0%F	Steel Strand	9.6	2900	0%	–	–
NSM-S-0%F-Sh				0%	CFRP Sheet	2900×100×0.17
NSM-S-50%F-Sh				50%		
NSM-S-60%F-Sh				60%		
NSM-S-70%F-Sh				70%		

Note: UB – unstrengthened beam; NSM – NSM strengthening technique; S – strengthened with steel strand; F – percentage prestressing force applied on strands; Sh – CFRP Sheet; EBR – EBR strengthening technique.

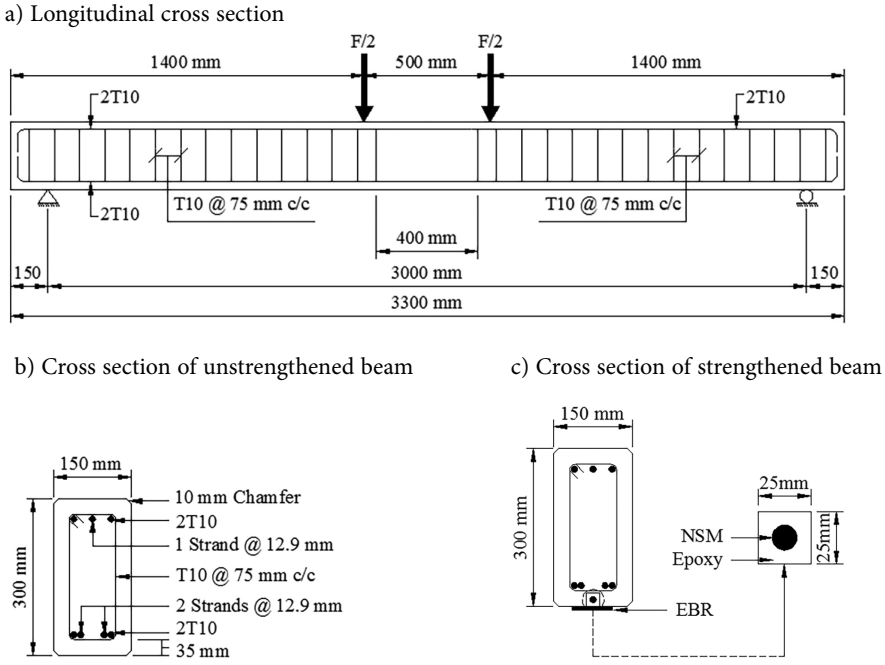

Figure 1. Specimen reinforcement details

1.3. Material properties

The beams were cast using high strength concrete, with ordinary Portland cement, natural sand as fine aggregate and crushed granite as coarse aggregate. The 28-day average compressive strength and flexural strength were 50 MPa and 5.5 MPa, respectively, based on concrete cube and prism tests conducted in accordance with the standards BS-EN-12390-3:2019 (British Standards Institution [BSI], 2009a) and BS-EN-12390-5:2019 (BSI, 2009b). The elastic modulus was 33.80 GPa. During prestress transfer from the internal prestressing strands to the concrete, the concrete compressive strength was 35 MPa.

Deformed 10 mm steel bars, with 500 MPa tensile strength and 200 GPa elastic modulus, were used for the main rebar and shear link. The internal prestressed strands and the NSM prestressed strands were seven wire low relaxation Grade 270 prestressing strands of 12.9 mm and 9.6 mm diameters, respectively, and 1860 MPa tensile strength and 195 GPa elastic modulus.

SikaWrap 301C woven unidirectional carbon fiber sheet of 0.167 mm thickness and 1.8 g/cm^3 density was used as the EBR material. The tensile strength, elastic modulus and ultimate strain of the sheet were 4900 MPa, 230 GPa and 1.7%, respectively.

Two epoxy adhesives, Sikadur® 30 and Sikadur® 330, were used to bond the NSM strand and EBR sheet, respectively, to the concrete substrate. For Sikadur® 30 the compressive strength, tensile strength, shear strength, bond strength with concrete and elastic modulus were 95 MPa, 31 MPa, 19 MPa, 4 MPa and 11.2 GPa, respectively (Sikadur®-30, 2019). For Sikadur® 330 the tensile strength, elastic modulus, ultimate strain and bond strength with concrete were 30 MPa, 3.8 GPa, 0.9% and 4 MPa, respectively (Sikadur®-330, 2019).

1.4. Strengthening procedure

Strengthening was done after the 28-day concrete curing period. Five strengthening techniques were used in this study, namely EBR, NSM, PNSM, CEBNSM and CEBPNSM.

For the EBR technique, a CFRP sheet 2900 mm long by 100 mm wide and 0.167 mm thick was used. The concrete surface of the beam soffit was first prepared by grinding, blasting and appropriate cleaning to ensure proper bonding. The epoxy adhesive, Sikadur®330, was used to bond the CFRP sheet to the prepared concrete surface following the standard dry lay-up practice and allowed to cure for seven days.

For the NSM technique, one steel prestressing strand, 9.6 mm in diameter, was used. A single groove, 25 mm wide by 25 mm deep, was cut longitudinally along the soffit of the beam, and then roughened and cleaned appropriately to ensure proper bonding. The groove was then two-thirds filled with epoxy (Sikadur® 30), and the steel strand gently pressed into the epoxy, while ensuring a minimum of 10 mm clear cover from the soffit of the beam. The groove was then completely filled with more epoxy and allowed to cure for seven days. The bonded length was 2900 mm (200 mm from each side of the beam).

The PNSM technique was used before the EBR technique in the CEBPNSM strengthened beams, not independently on any beam in this study. For the PNSM technique, the steel strands were first prestressed in a special prestressing setup before placement in the epoxy filled groove. This setup consisted of a steel frame, clamps, anchors, hydraulic jack and an electric motor for lifting and positioning the beams, as can be seen in Figure 2. The beam with the NSM groove facing upwards was first placed in the frame and aligned to the anchors and hy-

a) During prestressing (dead end anchor)

b) After prestressing (live end hydraulic jack)

Figure 2. Prestressing system

draulic jack. The steel strand was then passed through the hydraulic jack and anchors, tightly clamped in place at the dead end, prestressed using the hydraulic jack at the live end to the desired level of prestress (50%, 60% or 70%), and then the hydraulic jack and live end anchor were tightly clamped to lock in the prestressing force. The NSM groove was then two-third filled with epoxy and then the beam was slightly raised in the frame using the electric motor and positioned to cause the prestressed steel strand to press into the epoxy filled groove, while ensuring a 10 mm clear cover from the beam soffit. Additional epoxy was used to completely fill the groove and the strengthened beam was then left in this condition to cure for six days. After six days, the prestressing force was gradually released by slowly loosening the clamp anchors and hydraulic jack to transfer the prestressing force through the epoxy to the beam, and then the steel strand was cut along the beam sides and the beam was allowed to cure for one more day. No cracks or damage to the beams were observed at the release of prestress.

For the CEBNSM technique, an NSM steel strand was used first to strengthen the beam, after which it was allowed to cure for seven days and then a EBR CFRP sheet was applied over the NSM strengthening, each following the procedures stated above. The CEBPNSM technique followed the same procedure as the CEBNSM technique, except that PNSM was used in the place of NSM, following the procedures for PNSM stated above. All strengthened beams were allowed to cure for at least seven days before testing.

1.5. Instrumentation and experimental setup

The specimens were tested under four-point static loading using a Universal Instron machine. The loading was controlled to 5 kN/min up to yielding of the specimens, after which displacement was controlled to 1.5 mm/min until complete failure. Deflection at midspan was measured with a 100 mm Linear Variable Differential Transducer (LVDT) until near failure after which manual measurement was done using a ruler. Two strain gauges, 5 mm in length, were fixed to the internal steel strands and the NSM steel strand at midspan during beam casting and strengthening to measure tensile strains. A 30 mm strain gauge was fixed to the top fiber of the beam at midspan to measure compressive strains. A portable data logger was use to capture the data from the load cell, LVDT and strain gauges. Crack width was measured at the soffit of the beam under the internal tension steel reinforcement using a digital microscope. The instrumentation and experimental setup can be seen in Figure 3.

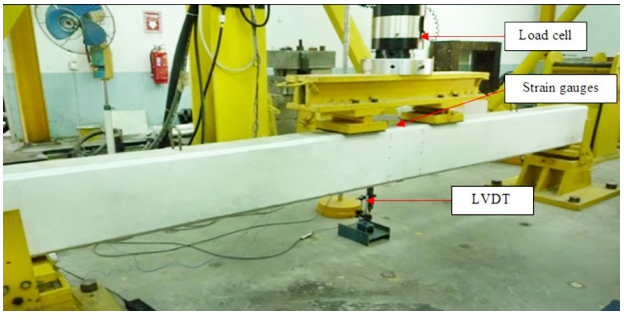

Figure 3. Instrumentation and layout of the experimental setup

2. Results and discussion

2.1. Flexural capacities

The flexural capacities of the beam specimens in terms of first crack, serviceability, yield and ultimate loads are displayed in Table 2. Overall, strengthening enhanced the flexural capacities of the beams at all load stages, with the CEBPNSM strengthened beams with higher levels of prestress showing the greatest enhancement. The first crack load improved by about 40% to 50% in the CEBPNSM strengthened beams, which is significantly higher than the other strengthened beams (about 5% to 15% improvement). The serviceability load was determined as the load corresponding to the deflection that is equal to span/480, as provided in ACI 318-11 (American Concrete Institute, 2011). This deflection was calculated to be 6.25 mm and the corresponding serviceability load in the control beam was 83 kN. The serviceability load improved by about 37% to 46% in the CEBPNSM strengthened beams, significantly more than the other strengthened beams (about 10% to 18% improvement). The yield load significantly improved by about 55% to 62% in the CEBPNSM beams. The use of the NSM steel strand greatly enhanced yield capacity due the superior yield properties of steel (Kim, 2010). The ultimate load showed the greatest improvement with about 65% to 70% increase in the CEBPNSM beams. From Figure 4, it can be clearly seen that the CEBPNSM technique and increasing the prestress level in the steel strand significantly enhanced the load capacities of the strengthened beams. The CEBPNSM strengthened beam with the highest level of prestress (70%) showed the greatest improvement, with increases of 31% in first crack load, 24% in serviceability, 21% in yield load and 8% in ultimate load, over the CEBNSM strengthened beam.

2.2. Failure modes

The typical failure modes of the beam specimens are displayed in Figure 4 and stated in Table 2. All the beam specimens had flexural failure modes. The control beam failed by typical concrete crushing failure in the maximum compression zone at the top face of the beam. The EBR CFRP sheet strengthened beam failed after yielding of the internal steel by concrete crushing followed by debonding of the CFRP sheet. As the concrete crushing occurred in the maximum compression zone, microcracks developed at the CFRP sheet and concrete interface, and the CFRP sheet lost full compatibility with the concrete surface and suddenly and swiftly debonded with a large explosive sound. The NSM strengthened beam failed by concrete crushing in the top compression zone after yielding of the internal steel, similar to the control beam. The CEBNSM and CEBPNSM strengthened beams failed by CFRP rupture in combination with concrete crushing after the tension reinforcement yielded. Concrete crushing initiated before rupture of the CFRP sheet and continued after CFRP rupture. The rupture of the CFRP sheet occurred in the maximum flexural zone and was accompanied by a loud sound. No debonding of the NSM steel strand or the CFRP sheet was observed. The failure behavior of the CEBNSM and CEBPNSM beams indicates the full composite action of the beams until failure and thus the full utilization of the tensile strength of the steel strand and CFRP sheet. Similar failure modes were also found by previous researchers using similar strengthening techniques, such as Darain et al. (2016), Obaydullah et al. (2016), Nordin and Täljsten (2006), Badawi and Soudki (2009) and El-Hacha and Gaafar (2011).

Table 2. Test results for load and deflection

Beam specimens	Level of Prestressing in NSM (%)	First Crack (P_{cr})		Serviceability Load (Ps) (kN)	Yield (P_y)		Ultimate load (P_{ult})		Failure Mode
		Load (kN)	Deflection (mm)		Load (kN)	Deflection (mm)	Load (kN)	Deflection (mm)	
UB	–	63.2	3.07	83.1	110.35	19.8	126.9	45.6	Concrete crushing
EBR-Sh	–	69.8 (10.5%)	3.18	92.6 (11.4%)	118.1 (7%)	9.7	165.3 (30.3%)	48.6	Concrete crushing
NSM-S-0%F	0	66.1 (4.7%)	3.17	91.7 (10.3%)	145.4 (31.8%)	23.5	161.9 (27.6%)	38.3	Concrete crushing
NSM-S-0%F-Sh	0	72.2 (14.3%)	3.16	98.3 (18.3%)	148.6 (34.6%)	14.5	200.3 (57.9%)	37.1	CFRP rupture
NSM-S-50%F-Sh	50	87.1 (37.9%)	3.12	113.5 (36.5%)	171.1 (55.1%)	13.5	209.8 (65.4%)	35.1	CFRP rupture
NSM-S-60%F-Sh	60	91.3 (44.5%)	3.08	116.3 (40%)	175.4 (59%)	13	212.9 (67.8%)	33.2	CFRP rupture
NSM-S-70%F-Sh	70	94.3 (49.3%)	2.50	121.70 (46.4%)	179.3 (62.5%)	12.7	216.1 (70.3%)	30.1	CFRP rupture

Note: Parentheses represents percentage increase over control beam.

a) Control beam (UB)

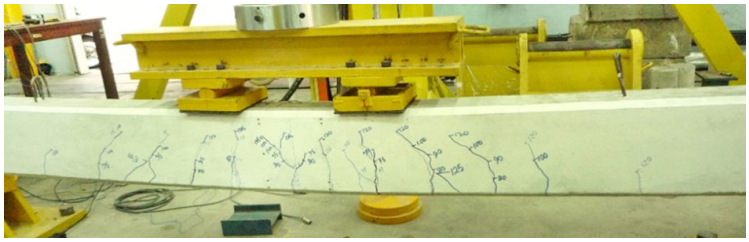

b) Typical failure mode of CEBPNSM beams (NSM-S-70%F-Sh)

Figure 4. Failure modes

2.3. Load-deflection behavior

The load-deflection curves of the beam specimens are presented in Figure 5 and the exact deflection values at first crack, yield and ultimate given in Table 2. Strengthening generally reduced overall deflection until ultimate due to increased beam stiffness, resulting in steeper load-deflection curves for the strengthened beams.

The control beam displayed typical elastic-plastic load-deflection behavior, with a steep linear elastic progression and minimal deflection until first crack, after which deflection gradually increased at a gentle slope until yield. From yield to ultimate, deflection increased rapidly and the load-deflection curve grew more inclined. After ultimate, deflection continued to increase, although load capacity slowly decreased, resulting in a gentle downward slope until beam collapse. The NSM beam displayed a ductile load-deflection response very similar to the control beam, except that a significantly higher curve was observed due to the increased yield and ultimate loads. The EBR beam displayed the typical tri-linear load-deflection response of CFRP strengthened beams (Rezazadeh et al., 2014). The deflection at yield was significantly less than the control beam due to the high stiffness of the CFRP, which significantly controlled deflection during service (before yield). After ultimate, the load abruptly fell back to the level of the control beam.

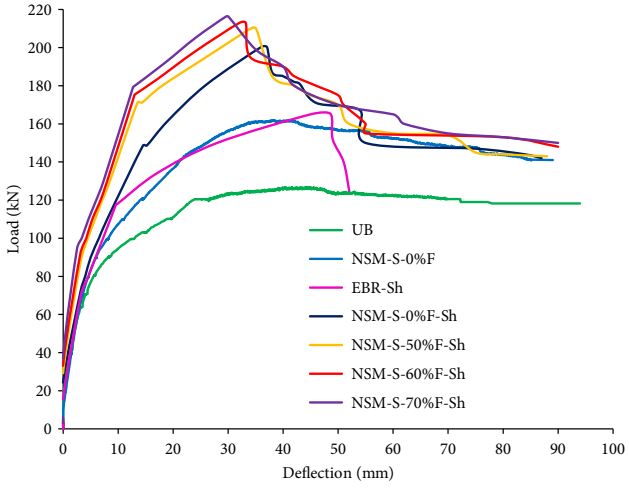

Figure 5. Load-deflection curves of the specimens

The CEBPNSM and CEBNSM strengthened beams also displayed similar tri-linear load-deflection responses, but with much higher yield and ultimate loads, and thus steeper curves with less deflection. This was due to the combined effect of the CFRP sheet and steel strand with the superior yield properties of steel greatly enhancing the yield point and the high stiffness of CFRP reducing deflection. The increased amount of strengthening material also resulted in greater beam strength and stiffness, and thus a higher ultimate and less deflection. The additional prestress in the steel strands in the CEBPNSM beams further increased strength and stiffness, resulting in significantly steeper and higher slopes at all stages until ultimate. The 70% prestress CEBPNSM beam showed the greatest enhancement in flexural response and reduction in deflection. The CEBPNSM strengthened beams were able to control and reduce deflection at first crack, yield and ultimate significantly more than the other strengthened beams, while simultaneously greatly increasing these load capacities. After CFRP rupture, the CEBPNSM and CEBNSM beams entered a degradation phase where the load-deflection response of the beams became erratic with

several sharp drops in loading and large deflections, until the beam fell back to the level of the NSM steel strengthened beam. The beam behavior was then governed by the combined strength remaining in the NSM steel and internal steel reinforcements until complete failure.

2.4. Cracking characteristics

The beams showed typical crack patterns, as seen in Figure 4. Strengthening improved first crack load, crack width, crack number and crack spacing. New cracks occurred from first crack until yield, after which no new cracks formed, although existing cracks widened and lengthened. The strengthened beams displayed more cracks, and smaller crack widths and crack spacing. No longitudinal cracks or shear cracks were seen at the soffit or the sides of the strengthened specimens, indicating full composite action between the beams and the strengthening materials.

The first crack loads and corresponding deflections are given in Table 2, and the increase in first crack load of the strengthened beams over the control beam is graphically presented in Figure 4a. The CEBPNSM strengthening technique was able to enhance the first crack load significantly more than the other strengthening techniques, due to the enhanced stiffness of the CEBPNSM beams in the pre-cracking stage. The CEBPNSM beam with the highest level of prestress (70%) showed the greatest increase in first crack load, 49% over the control beam, while also greatly reducing the deflection at first crack.

The first crack appeared in the constant moment zone for all the beams and the width of this crack was measured throughout testing. The correlation between load and crack width is shown in Figure 6a. Strengthening overall increased the load for a given crack width, with the CEBPNSM beams showing the greatest increases, as can be seen in Figure 6b. At 0.1 mm crack width, the CEBPNSM beam with 70% prestress carried a load of 160 kN, which was an increase of 56% over the control beam (102 kN), and an increase of 24% over the CEBNSM beam (129 kN). Crack width at service is an important design consideration. Strengthening was generally able to increase the serviceability (SLS) load while controlling crack width. The CEBPNSM beam with 70% prestress was able to increase the service load by 46% while decreasing crack width by 17%, compared to the control beam. The CEBPNSM technique was able to control crack width significantly better than the other strengthening techniques, with the 70% prestressed beam displaying the smallest crack width among the strengthened specimens.

Improved cracking behavior is highly advantageous as it reduces deflections and crack widths, improving the serviceability and durability of structures. The greatest improvement was seen in the CEBPNSM strengthened beams, especially with the higher levels of prestress. This was due mainly to the enhanced strength and stiffness of the beams from the greater amount of strengthening reinforcement and the opposing compressive forces provided by the additional prestress force in the steel strand.

a) Load vs crack width

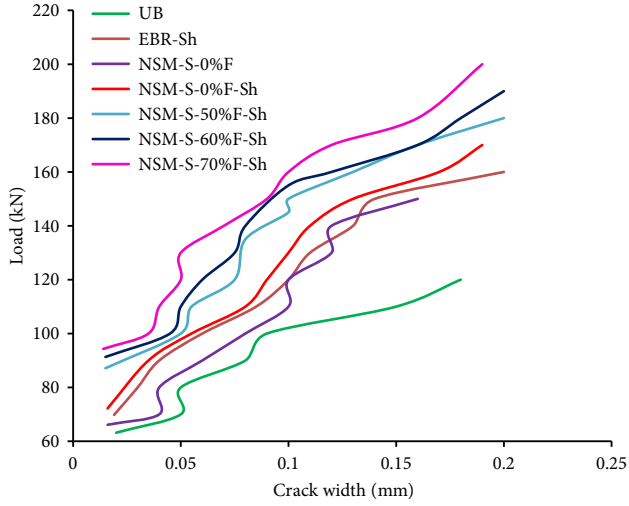

b) Load at 0.1 mm crack width

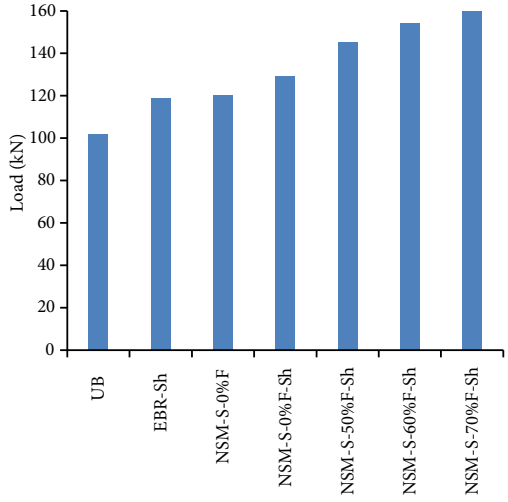

c) Crack width at SLS load

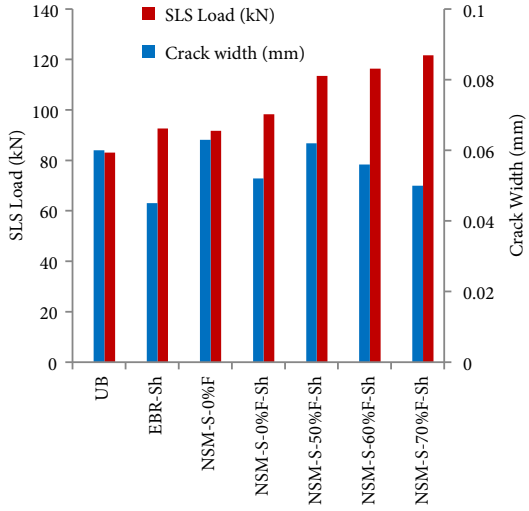

Figure 6. Crack width

2.5. Concrete compressive strains

The relation between loading and concrete compressive strain at midspan of the beam specimens is shown in Figure 7. The CEBPNSM strengthened beam with 70% prestress showed the greatest reduction in concrete compressive strain for a given load among the strengthened beams. This was due to the high level of prestress in the 70% beam which significantly enhanced the stiffness of the beam. The final strains measured in the beam specimens before the strain gauges were damaged by concrete crushing at failure were 0.00289, 0.00263, 0.00290, 0.00306, 0.00295, 0.00306 and 0.00295 in the control beam, NSM steel strand strengthened beam, EBR CFRP sheet strengthened beam, CEBNSM strengthened beam, and the 50%, 60% and 70% prestressed CEBPNSM strengthened beams, respectively. These final concrete strain values indicate that the full concrete strength of the beams was utilized, as concrete crushing occurs at a compressive strain value of around 0.003. This also indicates the full composite action of the strengthened beams until failure.

2.6. Tensile strains in main steel strands

The relation between loading and tensile strain in the bottom main strands is shown in Figure 8. The maximum tensile strain values measured before beam failure were 0.00612, 0.00842, 0.00705, 0.00752, 0.00721, 0.00701 and 0.00691 for the control beam, NSM beam, EBR beam, CEBNSM beam, and the 50%, 60% and 70% CEBPNSM beams, respectively. The control beam had the lowest maximum tensile strain as it failed by concrete crushing at a much lower load level than the strengthened beams. The CEBNSM strengthened beam displayed a maximum tensile strain value that was between the maximum tensile strain values of the NSM and EBR strengthened beams, indicating that the tensile strain was distributed between the main steel strands, the NSM steel strand and the CFRP sheet. The CEBPNSM strengthened beams with 50%, 60% and 70% prestress, displayed progressively lower maximum tensile strain values, due to the preexisting compressive strains introduced into the lower half of the beams by prestressing the NSM steel strand, which opposed the tensile strains created by loading. This is similar to the findings of El-Hacha and Gaafar (2011).

2.7. Tensile strains in NSM steel strands

The relation between loading and tensile strain in the NSM steel strands is shown in Figure 9. Prestressing caused an initial strain in the prestressed NSM steel strands used in the CEBPNSM strengthened beams. This initial strain was calculated from the effective prestressing force and the load-tensile strain curves of the prestressed NSM strands were thus accordingly displaced at zero loading, as can be seen in Figure 9. The maximum tensile strains in the NSM steel strands were 0.01521, 0.01100, 0.01277, 0.01255 and 0.01245 for the NSM beam, the CEBNSM beam and the CEBPNSM beams with 50%, 60% and 70% prestress, respectively. The CEBNSM strengthened beam had the lowest maximum tensile NSM steel strand strain, lower than the CEBPNSM beams as no initial strain was present in the NSM steel strand. However, the CEBPNSM strengthened beams showed the least increment in strain from load initiation until failure. Specifically, the CEBPNSM

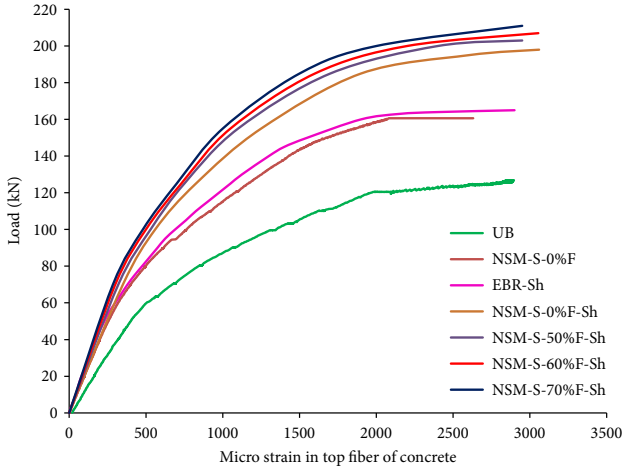

Figure 7. Load versus concrete compressive strain of beam specimens

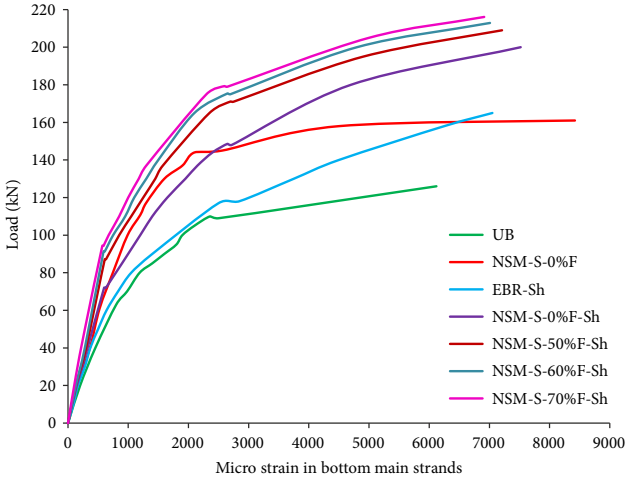

Figure 8. Load versus tensile strain in bottom main strands

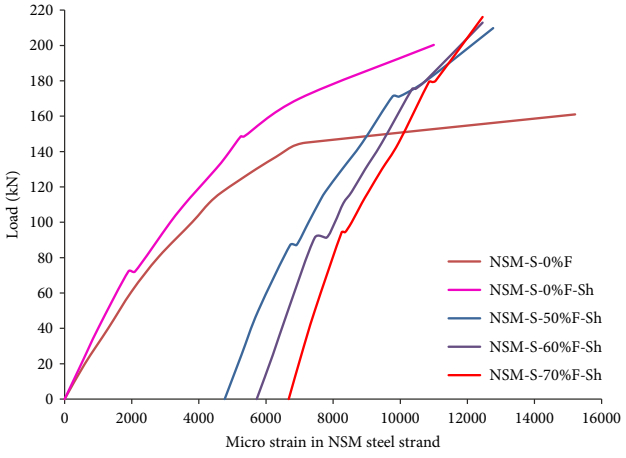

Figure 9. Load versus tensile strain in NSM strand

beam with 70% prestress showed the least increment in tensile NSM strand strain, only 0.00578 (this disregards the initial strain from prestress). The addition of prestress and the consequent compression around the NSM strand is the probable cause of this behavior.

2.8. Tensile strains in the CFRP sheet

The relation between loading and tensile strain in the CFRP sheets at midspan is shown in Figure 10. Each of the beams showed similar tri-linear tensile strain development in the CFRP sheet, with first crack, yield and ultimate marking the end of each phase. The maximum tensile strains measured in the CFRP sheets 0.01931, 0.02350, 0.02310, 0.02240 and 0.02201 for the EBR beam, CEBNSM beam and the 50%, 60% and 70% CEBPNSM beams, respectively. The rupture strain of the CFRP sheet was 0.02130, based on the manufacturer's specifications. The EBR strengthened beam had a lower maximum CFRP tensile strain as the CFRP sheet debonded at failure. The CEBNSM and CEBPNSM beams recorded tensile CFRP strains somewhat higher than the ultimate rupture strain provided by the manufacturer. This could be due to the local curvature of the CFRP at midspan, which may have caused the strain gauges to record higher strain values than those found in direct tensile tests (Rezazadeh et al., 2014). The maximum strains measured in the CEBNSM and CEBPNSM strengthened beams indicate that the full capacity of the CFRP sheet was utilized, which agrees with the observed failure mode of CFRP rupture and concrete crushing and confirms the full composite action of these strengthened beams.

2.9. Prestress losses

The prestressed NSM steel strands in the CEBPNSM strengthened beams were monitored for losses in prestress force from the time the prestress was applied until the release of the prestress into the beams. The amount of force applied to prestress the 50%, 60% and 70% prestressed CEBPNSM strengthened beams were 51.15 kN, 61.38 kN and 71.61 kN, respectively, which were calculated based on the tensile strength of the steel strands (Table 3). After the application of prestress to the steel strands, the strengthened beams were left locked in the prestressing setup for six days to allow the epoxy to cure fully. During this period, the prestressing forces in the steel strands were monitored using the hydraulic jack, and negligible losses in prestress were found as can be seen in Figure 11. The prestress losses were 0.47%, 0.54% and 0.36% in the 50%, 60% and 70% beams, respectively. When the prestressing forces were released, the effective prestress in the steel strands after prestress loss (Table 3) created an initial maximum strain in the steel strands of 0.00475, 0.00569 and 0.00665 for the 50%, 60% and 70% beams, respectively. The prestressing forces where released gradually into the beam around 20% at a time and no cracks were seen during or after prestress release. During prestress release, an LVDT was used to measure the negative camber at the midspan of the strengthened beams, which were found to be 0.05 mm, 0.06 mm and 0.07 mm for the 50%, 60% and 70% CEBPNSM beams, respectively.

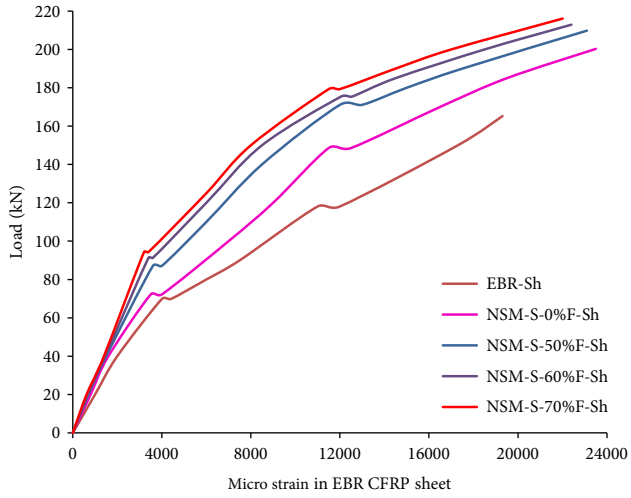

Figure 10. Load versus tensile strain in CFRP sheet

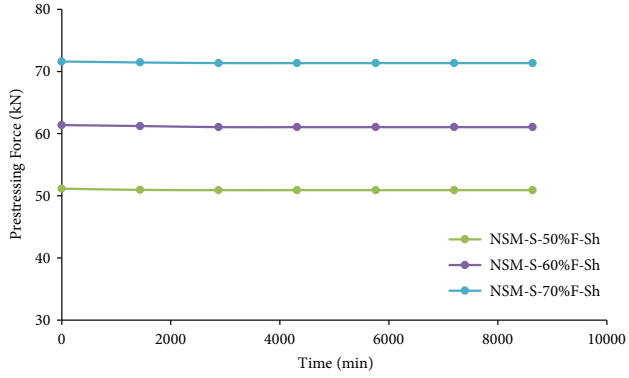

Figure 11. Prestressing force in steel strands during curing period

Table 3. Prestressing force and camber effect in the CEBPNSM strengthened beams

Beam ID	Applied Prestress Force		Effective Prestress Force		Negative Camber at Midspan
	(kN)	(%)	(kN)	(%)	(mm)
NSM-S-50%F-Sh	51.15	50.00	50.91	49.77	0.05
NSM-S-60%F-Sh	61.38	60.00	61.05	59.68	0.06
NSM-S-70%F-Sh	71.61	70.00	71.35	69.75	0.07

2.10. Influence of prestress level on flexural performance

Prestressing the NSM steel strand in the CEBPNSM strengthened beams had a significant effect on the flexural performance of the CEBPNSM beam specimens. The prestressing effect was especially enhanced by increasing the level of prestress force and the highest level prestress force (70%) offered the greatest enhancement in flexural behavior. Overall, increasing the level of prestress enhanced flexural behavior by increasing flexural load capacity and reducing deflection, crack width, concrete compressive strains and tensile strains in main steel, NSM strands and CFRP sheet at any given load level.

As can be seen from Figure 12a, the flexural load capacity of the beam at first crack, service, yield and ultimate was significantly improved by increasing the level of prestress, with yield load especially showing the most improvement, and the 70% prestress level providing the highest loads at all stages. From Figure 12b, it can be seen that the beams with prestress were able to maintain deflection at the same level as the beam without prestress despite the increases in load at first crack, service and yield. At ultimate, increasing the level of prestress significantly decreased deflection, with the 70% prestress level showing the smallest ultimate deflection. In Figure 12c, it can be seen that at first crack, service, and ultimate, the beams with prestress were able to control crack width to the same level as the beam without prestress despite the increases in load at these stages. At yield, prestressing caused crack width to increase slightly, which may be due to the large increase in yield seen in the beams with prestress compared to the beam without prestress. Increasing the level of prestress was able to control concrete compressive strains and tensile strains in the main steel, NSM steel strand and CFRP sheet to significantly higher load levels. The rates at which these strains increased were significantly reduced. This can be seen in the strain graphs (Figures 7 to 10).

Increasing the level of prestress force in the strengthening NSM steel strand improved the flexural behavior of the beams due to the increased compressive effect in tension region of the beams, which caused a corresponding increase in the stiffness of the beams, as well as an increase in the camber of the beams (Obaydullah et al., 2016).

a) Load vs level of prestressing force

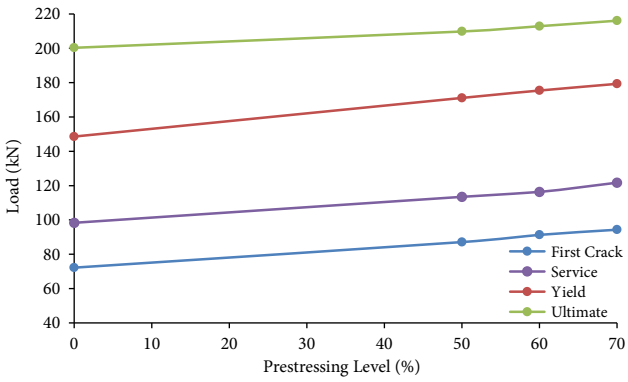

b) Deflection vs level of prestressing force

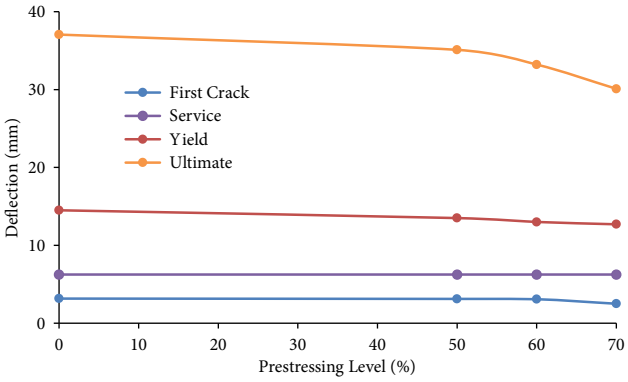

c) Crack width vs level of prestressing force

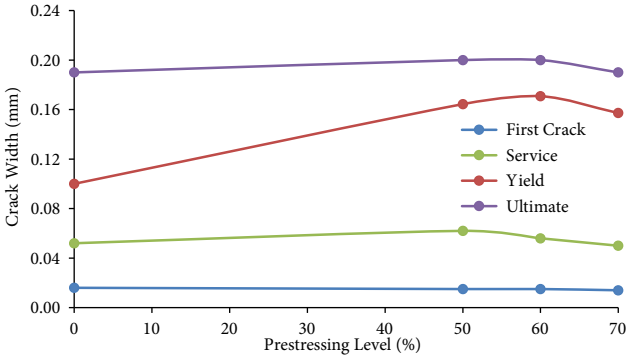

Figure 12. Effect of level of prestressing force

3. Finite element modelling

A 3D finite element model (FEM) was developed to perform numerical analysis in order to validate the experimental results. The models were developed and analyzed using ABAQUS. The failure mode, ultimate load and load-deflection behavior was modelled for the control beam, the beam strengthened with EBR CFRP sheet, the beam strengthened with a non-prestressed NSM steel strand, the CEBNSM strengthened beam with a NSM steel strand plus EBR CFRP sheet, and the CEBPNSM strengthened beams with 60% and 70% prestressed NSM steel strands plus EBR CFRP sheet.

The material characteristics, geometric dimensions, boundary and conditions of the modelled beams were identical to the experimental conditions. An 8-node linear solid element, C3D8R, was used to model the concrete and CFRP sheet. A 2-node straight truss element, T3D2, was used to model the steel reinforcements. To ascertain that the FEM models were able to accurately simulate the behavior of the beam specimens by appropriately transferring loads from one material to another, an appropriate meshing size was specified to discretize the concrete, steel, CFRP and epoxy, as can be seen in Figure 13c.

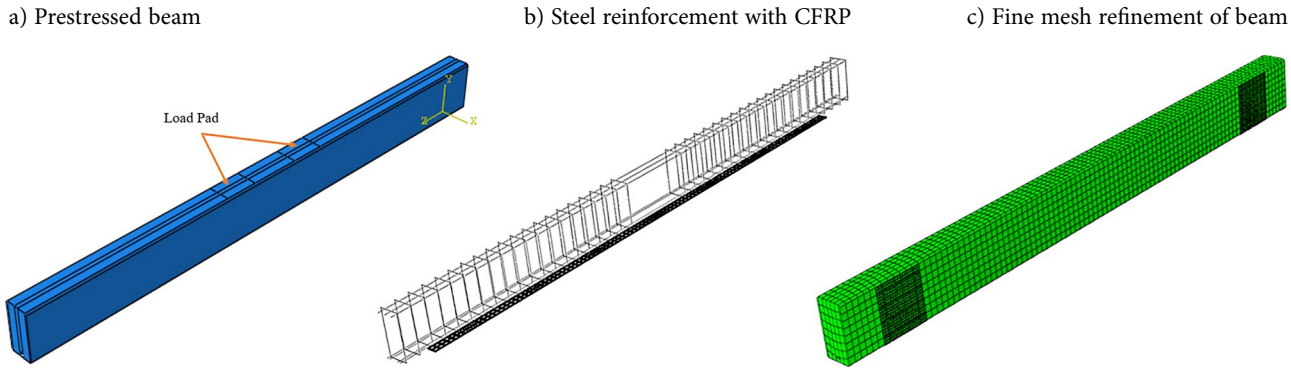

Figure 13. FEM model of prestressed beam

3.1. Modeling of materials

The concrete damaged plasticity model provided in ABAQUS was used to characterize the inelastic behavior of concrete in tension and compression as well as the damage characteristics of concrete. The model assumes that tensile cracking and compressive crushing are the main failure mechanisms. Elasto-plastic models were used to model the behavior of the steel and epoxy adhesive. An idealized isotropic hardening plasticity model was used to model the behavior of steel up to its ultimate tensile strength. The perfect plasticity model with no hardening was used to simulate the epoxy adhesive behavior. For the CFRP, a linear elastic stress to strain relation was adopted to simulate tensile behavior up to the ultimate tensile strength after which the contribution of the CFRP was neglected (Lee et al., 2017).

3.2. Modeling of interface bonds

In this study, three interfaces were considered. The first was that between the steel and concrete, the second interface was between the CFRP and epoxy, and the third interface was that between the concrete and epoxy. For this study, all of the interface bonds were assumed to be perfectly bonded. The tie and embedded constraints feature in ABAQUS was used to model these interface bonds. The steel reinforcement was considered as embedded inside the concrete and the CFRP sheet was considered as perfectly attached to the beam soffit. The epoxy was constrained to the concrete using tie constraints. The perfect bond model demonstrates some overestimation of ultimate load and stiffness compared to the experimental results. However, this approach is more convenient in terms of convergence and computation capability (Darain et al., 2016; Lee et al., 2017).

3.3. Modeling of prestress forces and loading

Three steps were adopted to simulate the internal prestressing, prestressed strengthening, and loading conditions of the beam specimens. Firstly, the prestressing forces in the internal prestressed strands were applied as 1395 MPa stress which is equivalent to 75% of the tensile strength of the main internal strands. Secondly, the prestressing force in the strengthening NSM steel strand was applied as an initial stress of 0 MPa for the beam with no prestressed strengthening, 930 MPa for the 50% prestressed strengthened beam, 1116 MPa for the 60% prestressed strengthened beam, and 1302 MPa for the 70% prestressed strengthened beam. Thirdly, the monotonic loading of the beams until complete failure was simulated as a uniform pressure force applied to the beam through two load pads (Figure 13a).

3.4. Assessment of FEM predictions with experimental results

Table 4 presents a comparison between the experimental and FEM results. A maximum 3% error for the ultimate load and 7% for corresponding deflections was found between the experimental and numerical results, which

Table 4. Comparison between experimental and FEM output at Ultimate load

Beam specimens	Level of Prestressing (%)	Experimental		FEM		FEM/Experimental	
		Load (kN)	Deflection (mm)	Load (kN)	Deflection (mm)	Load (PFEM/Pexp)	Deflection (ΔFEM/ Δexp)
UB	–	126.87	45.55	131.01	46.50	1.03	1.02
EBR-Sh	–	165.25	48.61	167.49	45.30	1.01	0.93
NSM-S-0%F	0	161.92	38.29	162.51	39.26	1.00	1.03
NSM-S-0%F-Sh	0	200.30	37.06	196.92	38.08	0.98	1.03
NSM-S-60%F-Sh	60	212.90	33.21	211.95	33.40	1.00	1.01
NSM-S-70%F-Sh	70	216.10	30.10	214.05	30.67	0.99	1.02

is well within the acceptable limit (10%) (Darain et al., 2016). Thus, a satisfactory agreement was found for load carrying capacity between the numerical FEM model and the experimental output.

The typical FEM and experimental load-deflection curves for the beam specimens are given in Figure 14. The FEM model was able to produce load-deflection curves for the beam specimens from the pre-cracking stage until failure. As can be seen from the graphs, the correlation between the numerical results and experimental data is reasonably good.

Figure 15 shows the pattern of damage behavior produced by the FEM model, for concrete compression and concrete tension. The concrete damage behavior was similar for all the modelled beam specimens. The ABAQUS software is unable to display compressive damage and tensile damage in the same frame, which is why they presented separately. Concrete beams typically fail by concrete crushing at the top fiber of the beam after the tension reinforcement yields. For beams strengthened using CFRP, flexural failure starts with some concrete crushing in the maximum compression zone, followed by CFRP rupture and more concrete crushing. All of the experimental beams experienced similar failure behavior. Thus, the numerical damage prediction of the beam specimens was consistent with the experimental failure behavior.

a) Load vs deflection for control beam (UB)

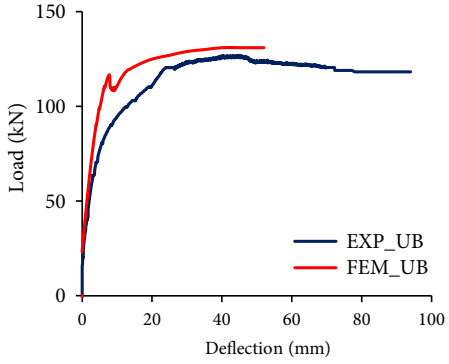

b) Typical load vs deflection for CEBPNSM beams (NSM-S-70%F-Sh)

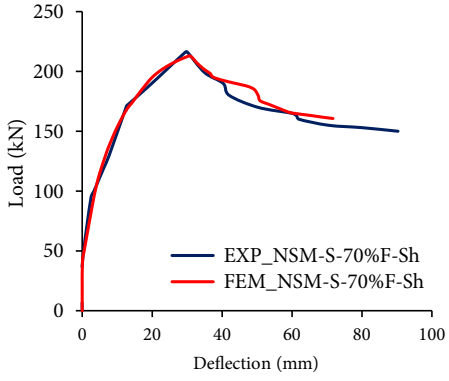

Figure 14. Load vs deflection curves of FEM and experimental beams

a) Concrete compressive damage behavior

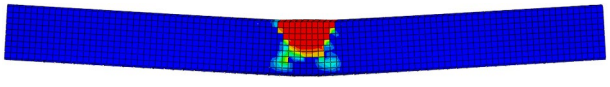

b) Concrete tensile damage behavior

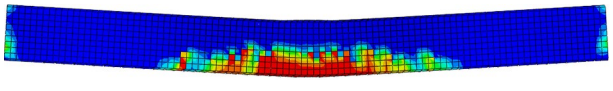

Figure 15. Damage behavior of beams

Conclusions

In this study four strengthening techniques were examined by experimentally testing the flexural behavior of seven prestressed concrete beams and developing a numerical FEM model to simulate the behavior of the beam specimens. The four techniques examined were the EBR technique, the NSM technique, the CEBNSM technique and the CEBPNSM technique, which were applied with the use of steel strands as NSM reinforcement and CFRP sheet as the external reinforcement. For the CEBPNSM technique, additional prestress force was also applied to the NSM steel strand. The main purpose of this study was to examine the newly proposed CEBPNSM strengthening technique and determine the capability of this technique to enhance the flexural behavior of prestressed concrete beams in comparison to other existing strengthening techniques. The following conclusions were derived from this study:

- The CEBPNSM technique was found to be an effective new strengthening technique for prestressed concrete beams. The CEBPNSM technique was able to greatly enhance the flexural performance of the prestressed concrete beam in terms of increased load carrying capacity at first crack, service, yield and ultimate, and reduced deflection, crack widths, compressive strains and tensile strains.
- The CEBPNSM strengthening technique significantly improved the flexural behavior of the beam when compared to the existing EBR, NSM and CEBNSM strengthening techniques. This can be attributed to the combination of materials and techniques, and the addition of prestress.
- Prestressing the NSM streel strand used in the CEBPNSM technique significantly improved flexural behavior compared to the beam strengthened with a combination of NSM and EBR but without prestress (CEBNSM).
- The higher the level of prestress, the greater the improvement in flexural behavior, with the highest level of prestress used (70%) showing the greatest improvement. Increasing the level of prestress especially enhanced load carrying capacity at first crack, service, yield and ultimate, and reduced deflection, crack width, and compressive and tensile strains at any applied load level.

– All of the strengthened beams except for the EBR strengthened beam, displayed flexural failure modes after yielding of the tension steel reinforcements. The CEBPNSM strengthened beams failed by CFRP rupture with concrete crushing, and no debonding or separation of the concrete cover was observed. This indicates the full composite action of the strengthened beams, which was further confirmed by the compressive and tensile strain measurements at failure.
– The FEM model produced ultimate load values for the beam specimens that were in decent agreement with the experimental results, with only a maximum 3% error. The load-deflection curves and the pattern of damage behavior produced by the numerical model had reasonably good correlation to the experimental load-deflection curves and failure modes.

This study has found that the CEBPNSM technique is an effective strengthening technique capable of fulfilling the service requirements of reinforced concrete structures and doing so more efficiently than other existing strengthening techniques. This strengthening technique may be able to provide a crucial advantage in the strengthening of structures. However, the prestressing system developed in this study is applicable only in the laboratory. Thus, further research work is essential to bring this technique to field application.

Acknowledgements

The researchers would like to gratefully acknowledge the financial support [Project No. GPF050A-2020, University of Malaya Research Grant-Faculty Programme] in conducting the research.

References

Al-Mahmoud, F., Castel, A., François, R., & Tourneur, C. (2009). Strengthening of RC members with near-surface mounted CFRP rods. *Composite Structures*, *91*(2), 138–147. https://doi.org/10.1016/j.compstruct.2009.04.040

American Concrete Institute. (2011). *Building code requirements for structural concrete* (*ACI 318-11*) *and commentary*.

Attari, N., Amziane, S., & Chemrouk, M. (2012). Flexural strengthening of concrete beams using CFRP, GFRP and hybrid FRP sheets. *Construction and Building Materials*, *37*, 746–757. https://doi.org/10.1016/j.conbuildmat.2012.07.052

Badawi, M., & Soudki, K. (2009). Flexural strengthening of RC beams with prestressed NSM CFRP rods–experimental and analytical investigation. *Construction and Building Materials*, *23*(10), 3292–3300. https://doi.org/10.1016/j.conbuildmat.2009.03.005

Brena, S. F., Bramblett, R. M., Wood, S. L., & Kreger, M. E. (2003). Increasing flexural capacity of reinforced concrete beams using carbon fiber-reinforced polymer composites. *Structural Journal*, *100*(1), 36–46. https://doi.org/10.14359/12437

British Standards Institution. (2009a). *Testing hardened concrete. Compressive strength of test specimens* (British Standard No. BS EN 12390-3:2019).

British Standards Institution. (2009b). *Testing hardened concrete. Flexural strength of test specimens* (British Standard No. BS EN 12390-5:2019).

Casadei, P., Galati, N., Boschetto, G., Tan, K. Y., Nanni, A., & Galecki, G. (2006, June). Strengthening of impacted prestressed concrete bridge I-girder using prestressed near surface mounted C-FRP bars. In *Proceedings of the 2nd International Congress* (pp. 5–8).

Darain, K. M. (2016). *Strengthening performance of reinforced concrete beam using combined externally bonded and near surface mounted techniques* [Doctoral dissertation]. University of Malaya.

Darain, K. M., Jumaat, M. Z., Hossain, M. A., Hosen, M. A., Obaydullah, M., Huda, M. N., & Hossain, I. (2015). Automated serviceability prediction of NSM strengthened structure using a fuzzy logic expert system. *Expert Systems with Applications*, *42*(1), 376–389. https://doi.org/10.1016/j.eswa.2014.07.058

Darain, K. M., Jumaat, M. Z., Shukri, A. A., Obaydullah, M., Huda, M., Hosen, M., & Hoque, N. (2016). Strengthening of RC beams using externally bonded reinforcement combined with near-surface mounted technique. *Polymers*, *8*(7), 261. https://doi.org/10.3390/polym8070261

De Lorenzis, L., & Nanni, A. (2001). Characterization of FRP rods as near-surface mounted reinforcement. *Journal of Composites for Construction*, *5*(2), 114–121. https://doi.org/10.1061/(ASCE)1090-0268(2001)5:2(114)

De Lorenzis, L., & Teng, J. G. (2007). Near-surface mounted FRP reinforcement: An emerging technique for strengthening structures. *Composites Part B: Engineering*, *38*(2), 119–143. https://doi.org/10.1016/j.compositesb.2006.08.003

El-Hacha, R., & Gaafar, M. (2011). Flexural strengthening of reinforced concrete beams using prestressed, near-surface-mounted CFRP bars. *PCI Journal*, *56*(4), 134–151. https://doi.org/10.15554/pcij.09012011.134.151

El-Hacha, R., & Rizkalla, S. H. (2004). Near-surface-mounted fiber-reinforced polymer reinforcements for flexural strengthening of concrete structures. *Structural Journal*, *101*(5), 717–726. https://doi.org/10.14359/13394

Hosen, M., Jumaat, M. Z., Alengaram, U. J., Islam, A. B. M., & Bin Hashim, H. (2016). Near surface mounted composites for flexural strengthening of reinforced concrete beams. *Polymers*, *8*(3), 67. https://doi.org/10.3390/polym8030067

Kim, Y. J. (2010). Flexural response of concrete beams prestressed with AFRP tendons: Numerical investigation. *Journal of Composites for Construction*, *14*(6), 647–658. https://doi.org/10.1061/(ASCE)CC.1943-5614.0000128

Lee, H. Y., Jung, W. T., & Chung, W. (2017). Flexural strengthening of reinforced concrete beams with pre-stressed near surface mounted CFRP systems. *Composite Structures*, *163*, 1–12. https://doi.org/10.1016/j.compstruct.2016.12.044

Lim, D. H. (2009). Combinations of NSM and EB CFRP strips for flexural strengthening of concrete structures. *Magazine of Concrete Research*, *61*(8), 633–643. https://doi.org/10.1680/macr.2008.61.8.633

Nordin, H., & Täljsten, B. (2006). Concrete beams strengthened with prestressed near surface mounted CFRP. *Journal of Composites for Construction*, *10*(1), 60–68. https://doi.org/10.1061/(ASCE)1090-0268(2006)10:1(60)

Obaydullah, M., Jumaat, M. Z., Alengaram, U. J., ud Darain, K. M., Huda, M. N., & Hosen, M. A. (2016). Prestressing of NSM steel strands to enhance the structural performance of pre-

stressed concrete beams. *Construction and Building Materials*, *129*, 289–301. https://doi.org/10.1016/j.conbuildmat.2016.10.077

Rahman, M. M., Jumaat, M. Z., Rahman, M. A., & Qeshta, I. M. (2015). Innovative hybrid bonding method for strengthening reinforced concrete beam in flexure. *Construction and Building Materials*, *79*, 370–378. https://doi.org/10.1016/j.conbuildmat.2014.12.081

Reza Aram, M., Czaderski, C., & Motavalli, M. (2008). Effects of gradually anchored prestressed CFRP strips bonded on prestressed concrete beams. *Journal of Composites for Construction*, *12*(1), 25–34. https://doi.org/10.1061/(ASCE)1090-0268(2008)12:1(25)

Rezazadeh, M., Costa, I., & Barros, J. (2014). Influence of prestress level on NSM CFRP laminates for the flexural strengthening of RC beams. *Composite Structures*, *116*, 489–500. https://doi.org/10.1016/j.compstruct.2014.05.043

Sharaky, I. A., Torres, L., & Sallam, H. E. M. (2015). Experimental and analytical investigation into the flexural performance of RC beams with partially and fully bonded NSM FRP bars/strips. *Composite Structures*, *122*, 113–126. https://doi.org/10.1016/j.compstruct.2014.11.057

Sikadur®-30. (2019). *Product data sheet-adhesive for bonding of strengthening reinforcement*. http://usa.sika.com/en/solutions_products/Construction-Products-Services/repair-protection-home/products/02a002/02a013/02a013sa06/02a013sa06sa05.html